

Fabrication of Polymeric Visual Decoys for the Male Emerald Ash Borer (*Agrilus planipennis*)

Drew P. Pulsifer¹, Akhlesh Lakhtakia¹, Mahesh S. Narkhede², Michael J. Domingue³,
Beverly G. Post¹, Jayant Kumar⁴, Raúl J. Martín-Palma⁵, Thomas C. Baker³

1. Department of Engineering Science & Mechanics, Pennsylvania State University, University Park,
Pennsylvania 16802, USA

2. Center for Advanced Materials and Department of Plastics Engineering, University of Massachusetts Lowell,
Lowell, MA 01854, USA

3. Department of Entomology, Pennsylvania State University, University Park, PA 16802, USA

4. Center for Advanced Materials and Department of Physics & Applied Physics,
University of Massachusetts Lowell, Lowell, MA 01854, USA

5. Department of Materials Science & Engineering, Pennsylvania State University,
University Park, Pennsylvania 16802, USA

Abstract

Through a bioreplication approach, we have fabricated artificial visual decoys for the invasive species *Agrilus planipennis*—commonly known as the Emerald Ash Borer (EAB). The mating behavior of this species involves an overflying EAB male pouncing on an EAB female at rest on an ash leaflet before copulating. The male spots the female on the leaflet by visually detecting the iridescent green color of the female's elytra. As rearing EAB and then deploying dead females as decoys for trapping is both arduous and inconvenient, we decided to fabricate artificial decoys. We used a dead female to make a negative die of nickel and a positive die of epoxy. Decoys were then made by first depositing a quarter-wave-stack Bragg reflector on a polymer sheet and then stamping it with a pair of matched negative and positive dies to take the shape of the upper surface of an EAB female. As nearly 100 artificial decoys were fabricated from just one EAB female, this bioreplication process is industrially scalable. Preliminary results from a field trapping test are indicative of success.

Keywords: bioreplication, conformal-evaporated-film-by-rotation method, electroforming, negative die, positive die, stamping

Copyright © 2013, Jilin University. Published by Elsevier Limited and Science Press. All rights reserved.

doi: 10.1016/S1672-6529(13)60207-3

1 Introduction

Agrilus planipennis, commonly known as the Emerald Ash Borer (EAB), is a metallic colored wood-boring beetle native to Asia which was introduced accidentally to the state of Michigan, USA in the 1990s^[1,2]. Since then, this beetle species has spread through many deciduous forests on both sides of the St. Lawrence Seaway^[1]. The species is now a major threat to ash trees in North America because the larval and pupal stages of its life cycle take place in the phloem and new sapwood of all species of ash trees^[2]. During its developmental stages, the EAB bores along these layers of a tree trunk and disrupts the transportation of water

and nutrients in the tree^[2]. It takes about two years for the tree to begin showing symptoms of the infestation, and many infested trees die within three years of the infestation^[1,2].

Entomologists have observed mating behavior whereby an overflying EAB male will pounce on an EAB female which is at rest on a brightly lit ash leaflet^[3,4]. This pouncing behavior is thought to be initiated by the identification of the female by the male who recognizes the iridescent green coloration^[5] of the female's elytra (hardened forewings constituting the shell of the beetle) contrasting to the background of the ash leaflet^[4]. This behavior has been initiated by pinning dead female specimen to ash leaflets, after washing

Corresponding author: Akhlesh Lakhtakia

E-mail: akhlesh@psu.edu

away any semiochemicals with a solvent, and observing overflying males pounce on the dead females. In this way, a dead female lures living males.

Although a trap for live EAB males can be produced by coating a dead EAB female with a spray-on adhesive material^[4], it is not an insignificant operation to rear large numbers of EAB for a comprehensive monitoring and/or eradication program. Current experience is that a large number of person hours are needed to rear a small number of the beetles. Moreover, dead EAB females often break on traps and need to be replaced mid-season, which would render any widespread program economically infeasible.

As the rearing of EAB and the subsequent deployment of dead females in traps is both arduous and inconvenient, we decided to replicate the upper surface of EAB females in a way that would allow us to produce visual decoys en masse for use in traps^[6]. To facilitate industrial scalability of the fabrication of artificial decoys, we developed a bioreplication^[7] technique which combines the use of a matched pair of negative and positive dies with a nanofabricated quarter-wave-stack Bragg reflector. The production of the negative die involved a two-step technique originally devised to cast multiple replicas of the corneal layer of a blow fly's compound eye^[8]. The complementary positive die was produced through two successive castings based on the negative die. Casting from the negative die was found to be necessary in order to achieve a close match between the positive and negative dies. As the EAB male's pouncing behavior is suspected to be initiated largely by the iridescent green color of the female's elytra, we produced a quarter-wave-stack Bragg reflector^[9] by spin coating^[10,11] alternating layers of poly(vinyl cinnamate) (PVCN) and poly(acrylic acid) (PAA) on a poly(ethylene terephthalate) (PET) sheet. The Bragg reflector was designed to produce peak reflectance at 550 nm wavelength with a relatively narrow bandwidth, in order to mimic the coloration of the EAB. The fabrication procedure used to produce the artificial EAB decoys is shown schematically in Fig. 1.

Here we present the entire process to produce multiple visual decoys from a single EAB female as well as results from a preliminary field test which demonstrate the effectiveness of the fabricated decoys. These visual decoys are made of commonplace polymers and their production employs unit operations—including physical

vapor deposition, electroforming, spin coating, casting, and stamping—that are widespread in industry.

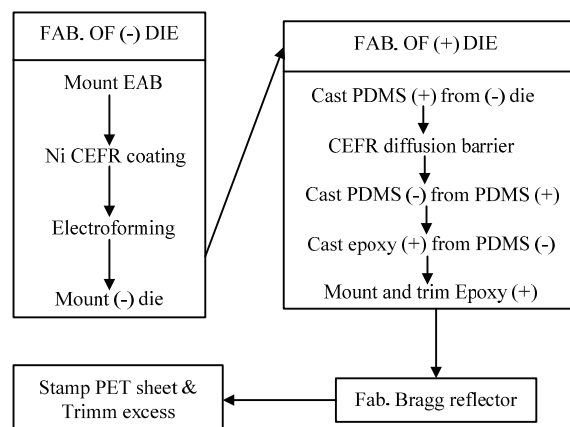


Fig. 1 Schematic outline of the process for producing a negative nickel die, a positive epoxy die, and a Bragg reflector all of which are then used to produce artificial visual decoys for use in traps for EAB males.

The plan of this paper is as follows. Section 2 is focused on the fabrication of the negative die, Section 3 contains a description of the procedure to fabricate the complementary positive die, and Section 4 deals with the production of the quarter-wave-stack Bragg reflector. The scalable production of visual decoys is presented in Section 5, and the results from a preliminary field test are provided in Section 6.

2 Fabrication of nickel negative die

2.1 Substrate preparation

A biotemplate, a dead EAB female, was mounted in polydimethylsiloxane (PDMS) on a glass slide which had a layer of kapton tape to serve later as a delamination layer. The mounting was done by placing the biotemplate on the slide and then pouring PDMS over it. Accordingly, a smooth transition was produced between the biotemplate and the slide, which is desirable (i) to eliminate areas that would be shadowed during the later deposition of nickel vapor on the biotemplate (Section 2.2) and (ii) to reduce overhangs when the resulting conformal coating of nickel would be reinforced by electroforming (Section 2.3). After the PDMS was cured, it was peeled away from the upper surface of the biotemplate's elytra and head to expose the surface of interest. Finally, the slide-mounted EAB specimen was sonicated in ethanol to remove any residue.

Fig. 2a shows a dead EAB female mounted on a glass slide with PDMS. Both elytra and the head are

exposed and will serve together with the PDMS mounting as a non-planar substrate for the deposition of a conformal coating of nickel.



(a)



(b)



(c)

Fig. 2 Production of a negative nickel die. (a) Photograph of a non-planar substrate comprising a dead EAB female mounted on a glass slide with PDMS. The PDMS mounting allows for a smooth transition between the biotemplate and the glass slide. (b) Photograph of the slide-mounted EAB female from (a) after being coated with ~ 500 nm of nickel in two successive CEFR runs. (c) Photograph of the electroformed negative die soldered into a steel ring and mounted to a stainless steel plate.

2.2 Conformal coating of nickel

In order to conformally coat the non-planar substrate, a modification of the Conformal Evaporated-

Film-by-Rotation (CEFR) method was adopted. The CEFR method involves the process of physical vapor deposition, and was originally developed to produce conformal coatings on non-planar substrates such as butterfly wings^[12] and fingerprints^[13]. It was modified for conformally coating highly lenticular substrates such as the eyes of insects^[14]. The modified CEFR method is implemented in a vacuum chamber containing both the substrate to be coated and a boat containing the material to be evaporated towards that substrate. A collimated vapor flux generated from the material is obliquely directed towards the substrate. Two programmable stepper motors allow a platform holding the substrate to be manipulated in order to produce a uniform coating.

On the surfaces of fly eyes, Pulsifer *et al.*^[14] have shown that the modified-CEFR method deposits coatings in which the standard deviation of thickness can be as little as 8% of the average thickness. As the EAB elytra are much flatter in comparison to fly eyes, the EAB elytra would be coated far more uniformly by the modified-CEFR method than the fly eyes.

For coating the EAB specimen, nickel was evaporated from a long and narrow boat made of tungsten. During deposition, the pressure in the vacuum chamber was maintained at $\sim 10^{-5}$ Torr and a current of ~ 90 A was passed through the boat to maintain a deposition rate of $1 \text{ nm}\cdot\text{s}^{-1}$. The substrate-holding platform was periodically rocked about a fixed axis in the platform plane through angles between 10° and 90° . Simultaneously, the platform was rotated about its surface normal at 120 rpm. The ~ 500 nm thick film of nickel was deposited in two successive CEFR runs, each run depositing ~ 250 nm of nickel. The use of two runs instead of just one run arose from the limited capacity of the tungsten boat. Any oxidation occurring on the nickel surface between the two runs did not have a deleterious effect on the second run.

Fig. 2b shows the slide-mounted biotemplate after being conformally coated with nickel. The upper surface of the nickel coating will later serve as a seed for the electroforming step, and the lower surface of the coating will later function as the active surface for stamping with the negative nickel die. Based on similar coatings on the eyes of insects^[8], the fidelity of bioreplication should be very good at the ~ 200 nm length scale, as the nickel coating should have grains not exceeding ~ 20 nm in maximum cross-sectional diameter.

However, nanoscale fidelity is not needed, as the scanning electron micrograph in Fig. 3a shows that the elytron has small-scale features at the $\sim 10\ \mu\text{m}$ length scale. Closer inspection of the elytron in Fig. 3b reveals the presence of $\sim 300\ \text{nm}$ diameter features which can best be described as pin holes. These pin holes do not appear in any ordered fashion or with sufficiently high frequency to substantially contribute to the optical response of the elytron. The scanning electron micrograph in Fig. 3c confirms that the negatives of the $\sim 10\ \mu\text{m}$ features are reproduced in the nickel coating.

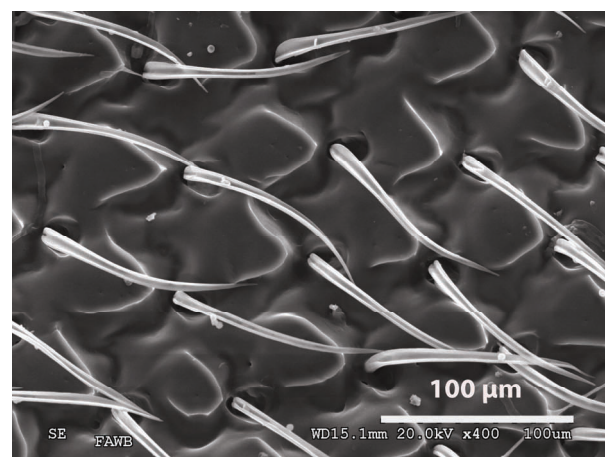
2.3 Electroforming

Electroforming is necessary to build up the nickel coating on the biotemplate in order to produce a negative die able to withstand the forces exerted when a polymer sheet is stamped^[15].

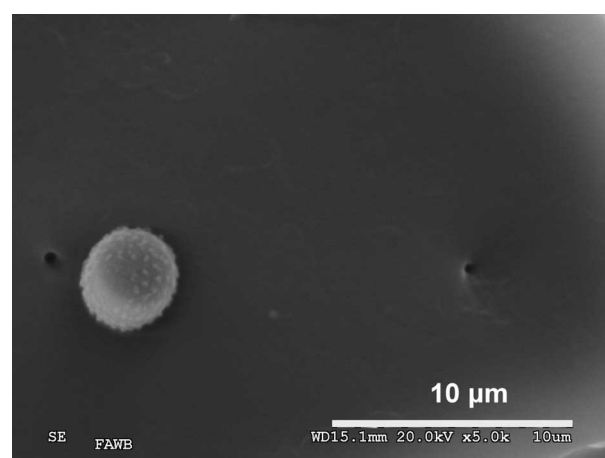
Electroforming of the nickel-coated biotemplate was carried out in a nickel sulfamate electrolytic solution that was mechanically agitated at room temperature. Three different electroforming stages of successively increasing electric current were implemented to minimize grain size at the working surface of the die while also allowing acceptable growth rates. During all three stages, the electroforming bath was maintained at $\sim 50\ ^\circ\text{C}$ for 2 days. The current was set at 20 mA for the first stage, 40 mA for the second, and 60 mA for the last stage. The electroformed layer produced was $\sim 100\ \mu\text{m}$ in thickness. After the electroforming step, the biotemplate was removed to leave behind a negative die of nickel.

2.4 Mounting of negative die

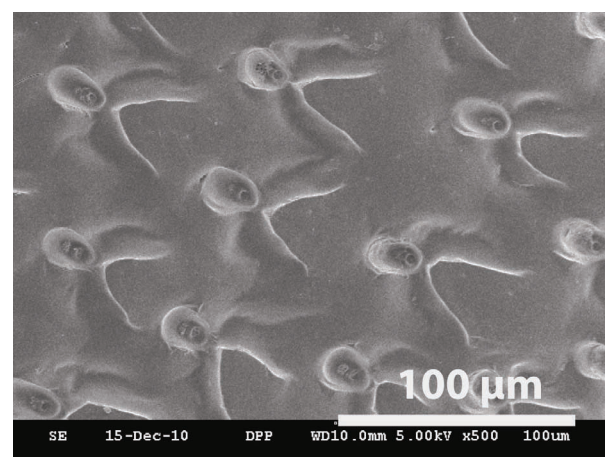
Although about $100\ \mu\text{m}$ thick, the electroformed nickel die has an irregular shape with the negative of the biotemplate protruding out of the plane of the majority of the die area. To facilitate the application of pressure that would be required to stamp polymer sheets, the negative nickel die was soldered into a steel ring. In this way the irregular shape of the nickel die was recessed into a solid fixture. The ring-mounted die was then attached to a stainless-steel sheet with an electrically insulating epoxy. The stainless-steel sheet will serve later as a heating element for the negative die when the decoys are stamped (Section 5). Fig. 2c shows the electroformed negative die soldered into a steel ring and attached to a stainless steel plate.



(a)



(b)



(c)

Fig. 3 Scanning electron micrographs of (a) the elytron of an EAB specimen at 400X magnification, (b) the same elytron at 5,000X magnification, and (c) the functional surface of the $\sim 500\ \text{nm}$ thick nickel coating at 500X magnification. As the surface of the coating is the negative of the elytron surface, the roots of the cilia on the elytron in (a) appear as elliptical depressions in (c). The micrograph (b) demonstrates the absence of ordered nanoscale features which could be involved in any optical effects.

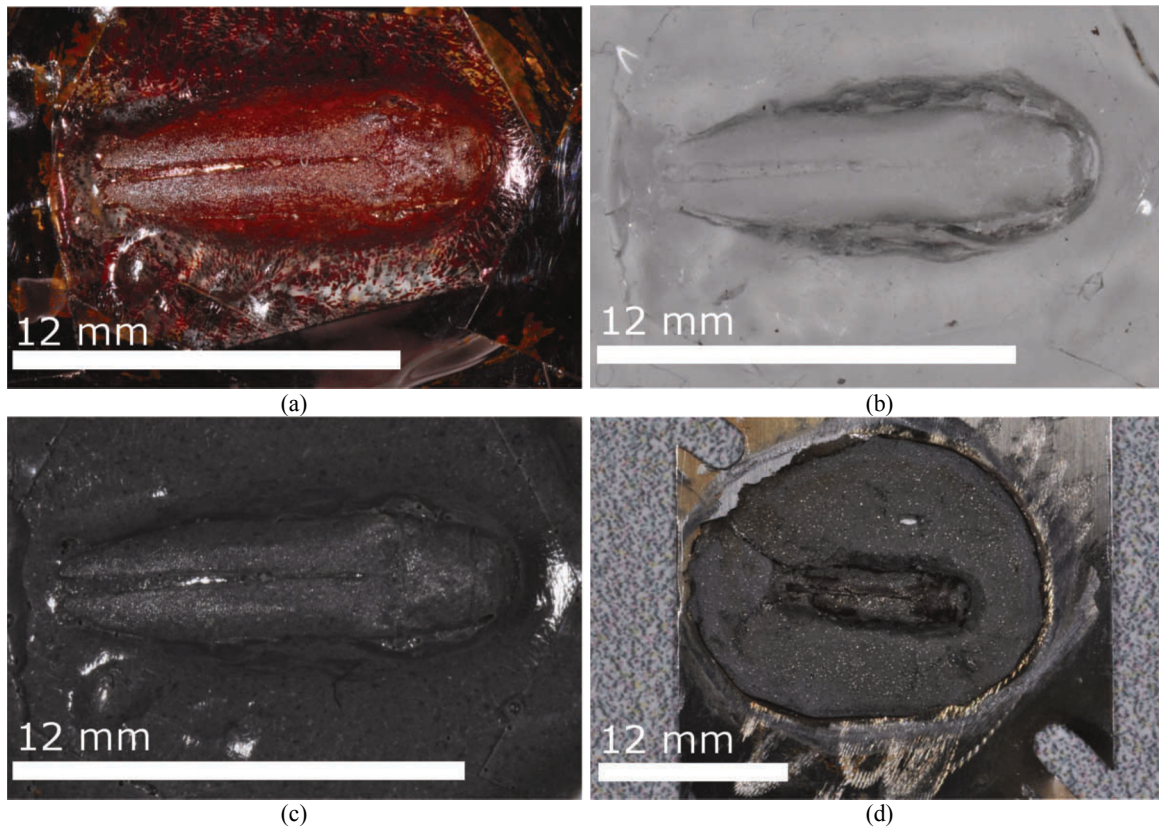


Fig. 4 Production of a positive epoxy die. (a) Photograph of the PDMS positive casting removed from the negative nickel die. The PDMS positive casting is coated with a 1000 nm thick coating of chalcogenide glass of nominal composition $\text{Ge}_{28}\text{Sb}_{12}\text{Se}_{60}$. (b) Photograph of the PDMS negative casting produced from the PDMS positive casting shown in (a). (c) Photograph of the positive epoxy die cast from the PDMS negative casting shown in (b). (d) Photograph of the positive epoxy die after mounting to a stainless-steel sheet and trimming to allow clearance for a PET sheet to be stamped.

3 Fabrication of epoxy positive die

The nickel negative die was filled with PDMS. After it was cured, the PDMS positive casting was removed from the nickel negative die, mounted to a glass slide with kapton tape, and then conformally coated with chalcogenide glass using the CEFR method. The resulting structure is presented in Fig. 4a.

The ~1000 nm thick coating of chalcogenide glass served simply as a diffusion barrier for the next step, wherein the structure shown in Fig. 4a was submerged in PDMS. After curing, the PDMS negative casting was pulled away from the PDMS positive casting. This PDMS negative casting, shown in Fig. 4b, is a close match of the nickel negative die.

The negative casting made of PDMS was then filled with an epoxy. Once the epoxy was cured, the PDMS negative casting was peeled away to leave behind a positive epoxy die of the biotemplate. This strategy was implemented to allow for the closest match possible between the positive and negative dies. The positive

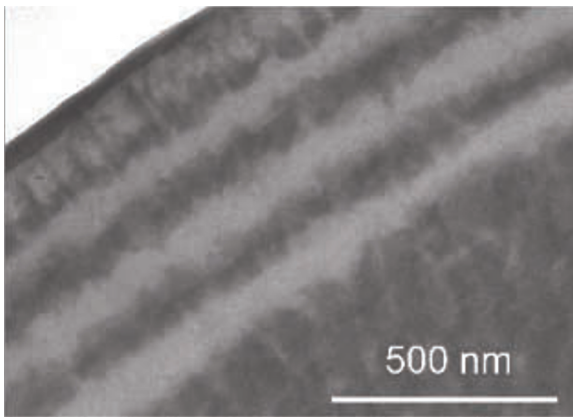
epoxy die was attached to a stainless-steel sheet for easy handling as well as heating during the stamping process (Section 5). Fig. 4c shows the epoxy positive die as it appears after removal from the PDMS negative casting. The epoxy in the positive die thus fabricated was trimmed to remove excess material and allow clearance for a PET sheet to be stamped. Fig. 4d shows the positive epoxy die which can be mated with the negative nickel die of Fig. 2c.

4 Fabrication of quarter-wave-stack Bragg reflector

The production of a PET replica of an EAB can be attempted by melting a PET sheet in the heated negative die and then pressing the positive die into the molten PET by hand^[6]. This process did not produce a satisfactory replica, for which reason we decided to mount the nickel negative die inside a sturdy metal ring on a stainless steel sheet. Equally significantly, the replica had a translucent white appearance, which would not lure any EAB male. This is because EAB elytra have an

iridescent green coloration produced by sub-cuticular stacking of quarter-wave layers, which is known from many beetle species to produce strong structural colors without the use of pigments^[9,16].

As is evident from the transmission electron micrograph shown in Fig. 5a, the outer region of the EAB elytron contains four bilayers, each comprising two ~135 nm thick layers of alternating refractive indexes. Thus the iridescent green coloration is produced by a quarter-wave stack Bragg reflector that develops during the pupal stage, and this coloration is not significantly disturbed by the presence of cilium-supporting ~70 μm dimples that can be seen in Fig. 3a. Reflectance spectrophotometric measurements show peak reflectance from EAB elytra to be close to 540 nm wavelength, quite similar to both ash leaflets and oak leaves and also similar to the elytra of *A. biguttatus*, an aggressive



(a)

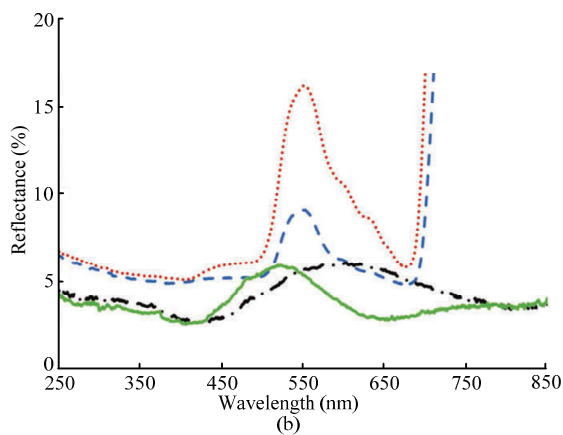


Fig. 5 (a) Transmission electron micrograph of a cross-section of a female EAB elytron, showing four alternating layers of differing refractive indexes and ~135 nm thickness; and (b) reflectance spectrophotometry profiles of the elytra of a female EAB, *A. planipennis* (solid green line) and an aggressive European oak-feeding species in the same genus, *A. biguttatus* (dash-dotted black line), compared to the reflectance profiles of an ash leaflet (dotted red line) and an oak leaf (dashed blue line).

European oak-feeding species; see Fig. 5b. Whether the EAB males are lured simply by the iridescent green coloration of the EAB females or also by the small-scale structures was an open question that we had also hoped to answer at the beginning of this project.

To mimic the natural Bragg reflector found in the EAB elytra, alternating layers of PVCN and PAA were spin-coated on one side of a $3 \times 3 \text{ cm}^2$ PET sheet. These polymers were chosen as their refractive indexes differ by 0.19, which is quite large. Furthermore, the solubilities of both polymers in orthogonal solvents are very different. PVCN (0.9 wt %) and PAA (1.2 wt %) solutions in chloroform and methanol, respectively, were used for spin coating. Bragg stacks were fabricated by consecutively coating 15 bilayers of PAA and PVCN at 1500 rpm. Since PAA and PVCN are insoluble in chloroform and methanol, respectively, the addition of a new layer via spin coating did not damage prior layers. A 15-bilayer Bragg reflector was selected over the 4-bilayer Bragg reflector found on EAB elytra in order to accentuate the iridescent coloration of the decoys.

The transmission spectrum of the resulting PET sheet with a quarter-wave-stack Bragg reflector is shown in Fig. 6a. These measurements were performed using a Perkin–Elmer Lambda-9 spectrophotometer, with an uncoated PET sheet as a reference. The transmission spectrum was collected using a spectrophotometer with a beam of $5 \times 3 \text{ mm}^2$ cross-sectional area. As the quarter-wave-stack Bragg reflector was fabricated with a spin coating process, which tends to produce layers which are thicker at the edges, the Bragg reflectors deposited on the PET sheets exhibit variation in their central wavelength. But the EAB elytra also exhibit variation in color, both red- and blue-shifted from the characteristic 540-nm green. Hence, the variation in color resulting from the spin coating process was not expected to negatively impact the decoy's ability to attract EAB males.

Thereafter, the other side of the PET sheet was coated with black ink as an absorber layer in order to enhance the spectrally selective reflection. A photograph of the resulting PET sheet with a quarter-wave-stack Bragg reflector on one side and a black absorber layer on the other side is presented in Fig. 6b. The reflectance of the doubly coated PET sheet as a function of wavelength is shown in Fig. 6c. These two figures confirm the desired green coloration.

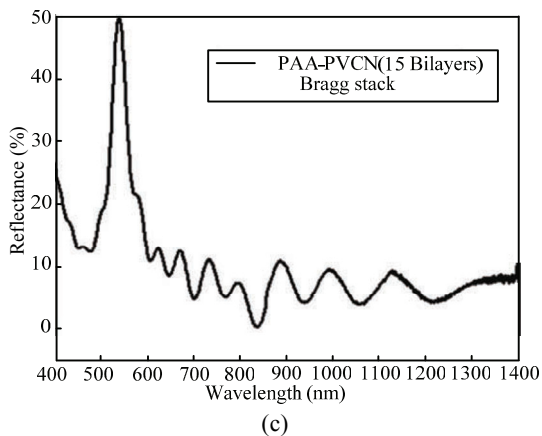
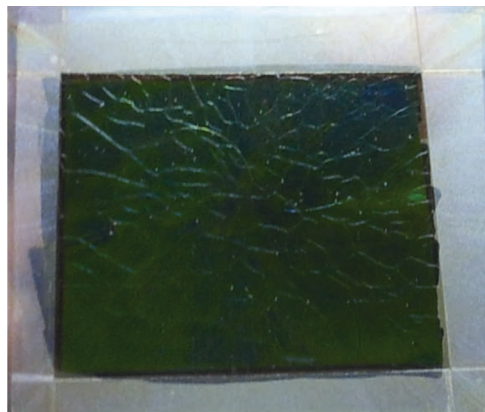
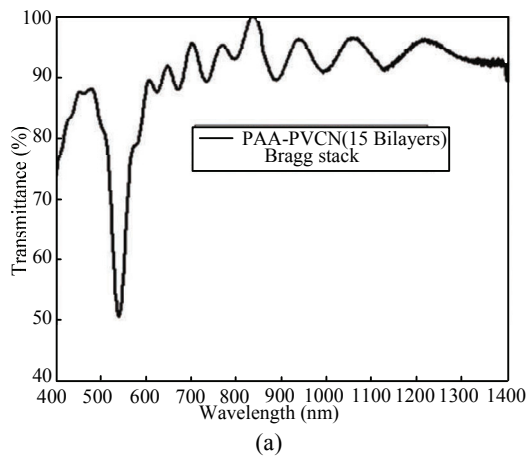


Fig. 6 (a) Measured transmittance spectrum of an unstamped PET sheet with a quarter-wave-stack Bragg reflector on one side but without a black absorber layer on the other side; (b) photograph of an unstamped PET sheet with a quarter-wave-stack Bragg reflector on one side and a black absorber layer on the other; and (c) measured reflectance spectrum of an unstamped PET sheet with a quarter-wave-stack Bragg reflector on one side and a black absorber on the other side.

5 Fabrication of visual decoys

Four types of visual decoys were fabricated to be tested against dead EAB females for the purpose of luring and trapping EAB males. An EAB female is

shown in Fig. 7a. The first type of visual decoy was simply a PET sheet, with a quarter-wave-stack Bragg reflector and an absorber layer, trimmed to resemble the silhouette of an EAB, as shown in Fig. 7b.

Visual decoys of the remaining three types were fabricated by hot stamping PET sheets, each coated with a quarter-wave-stack Bragg reflector on the upper side and a black absorber layer on the lower side, as described in Section 4. The PET sheet was pressed between the electrically heated positive and negative dies and allowed to cool under pressure. Once cooled, the now patterned sheet was removed from the dies and the excess material was trimmed away. Figs. 7c–7e show examples of the three types of visual decoys prepared in this way with some variation. The visual decoys exemplified by Fig. 7c were stamped with enough force to leave the general shape of the beetle and some surface details but do minimal damage to the quarter-wave-stack Bragg reflector. Visual decoys of the type shown in Fig. 7d were stamped more heavily in order to impart each decoy with the surface features of the EAB at the sacrifice of a portion of the Bragg reflector. Finally, visual decoys of the type shown in Fig. 7e were stamped heavily from a PET sheet which had a

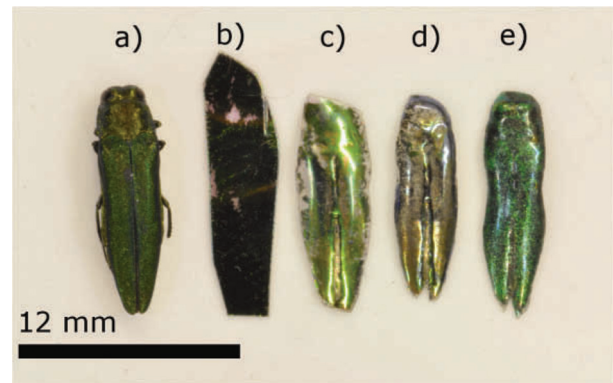


Fig. 7 (a) Photograph of a dead EAB female. (b–e) Photographs of visual decoys. (b) A PET sheet, with a quarter-wave-stack Bragg reflector and a black absorber layer, cut into a rough silhouette of an EAB. (c) A visual decoy produced by lightly stamping a PET sheet coated with a quarter-wave-stack Bragg reflector on the upper side and a black absorber layer on the lower side. Note that the quarter-wave-stack Bragg reflector is intact over much of the decoy. (d) A visual decoy produced similarly to the one shown in (c) but stamped more heavily. This yielded more fine features at the expense of area where little of the quarter-wave-stack Bragg reflector survived. (e) A visual decoy produced by heavily stamping a PET sheet with a quarter-wave-stack Bragg reflector, then painting the lower side first with emerald metallic paint and then a black absorber layer. Coloration found in (e) is primarily from the emerald metallic paint, as the Bragg reflector was destroyed by the heavy stamping.

quarter-wave-stack Bragg reflector on its upper side prior to stamping, but without a black absorber layer on its lower side. Following the heavy stamping, these visual decoys had their lower sides painted first with a commercially available metallic emerald green paint and then a black absorber layer. Coloration found in Fig. 7e is primarily from the emerald metallic paint, because the quarter-wave-stack Bragg reflector was destroyed by the heavy stamping.

6 Field tests

The color perceived by humans is not the same as spectral color (which is recorded by instruments)^[17]. Thus, the perceived green of EAB elytra depends not only on the reflectance in the green part of the spectrum but also on, among other factors, the relative reflectances at other wavelengths in the visible regime. The same is true of the perceived green of the quarter-wave-stack Bragg reflectors fabricated for this research. There is no unique correspondence between perceived color and spectral color (a phenomenon called metamerism), and there are wide variations in color perception in diverse human populations^[17]. As there are also wide variations in color perception by different mammals^[18], the color perceived by an insect would very likely differ from the color perceived by a human. Moreover, as perceived color is known to be affected in humans by motion^[19], color perception by a flying EAB male could be influenced by its motion. Hence, any definitive test of visual decoys requires their presentation to the subject species in the field.

Traps of five different types were prepared as follows: Traps of the first type contained a pinned dead EAB female each. Traps of the remaining types contained a visual decoy each, identified in Figs. 7b–7e. All visual decoys of types (c–e) originated from the same dead EAB female. Traps of types (a) and (b) served as control traps. About a hundred decoys of types (c–e) were made.

All of the traps were deployed in preliminary field tests conducted in June 2012. As the emergence of adult EAB in North America was premature in 2012 and because dead EAB females have been shown to work just as reliably in attracting a potentially destructive oak-feeding invasive pest species, *A. biguttatus*, as they do against EAB themselves^[20], we conducted *A. biguttatus* field trapping tests of the visual decoys in Hungary.

Although various types of field tests were conducted with different types of traps in different settings, one field test was conducted with an equal number of traps of all five types in the same setting to compare the effectiveness of traps containing visual decoys of types (c–e) against the control traps of types (a) and (b). Table 1 presents the data gathered from this field test and Fig. 8 shows a photograph of a trap which has captured an *A. biguttatus*.

Table 1 Data from a preliminary field test designed to compare the effectiveness of traps containing visual decoys of types (c–e) against control traps of types (a) and (b)

Type of luring agent in a trap	Number of traps deployed	Number of <i>A. biguttatus</i> males captured
(a)	6	4
(b)	6	1
(c)	6	5
(d)	6	5
(e)	6	7



Fig. 8 Photograph of a test trap with an *A. biguttatus* stuck to a visual decoy, thereby demonstrating that the polymeric visual decoys produced by us can initiate pouncing behavior. Field tests were conducted in Hungary.

Most of the other smaller insects caught in the traps were related insects of the same genus (*Agrilus*), who present a similar but less severe threat to forests. Also, many smaller insects were caught regardless of whether or not there are natural or artificial decoys. This is just a consequence of using a sticky trap, which many entomologists use all the time. Finally, this is also a problem of population density. There are hundreds if not thousands of times more of the smaller insects versus our target species, which all can be easily seen just by looking quickly at the trees for a moment.

The data in Table 1 show that visual decoys of types (c–e) performed better than the dead EAB females in attracting *A. biguttatus*. Moreover, the stamped visual decoys of all three types were much more successful in

luring overflying *A. biguttatus* than the unstamped visual decoys of type (b). This provides evidence that not only should a visual decoy have the same silhouette, size, and color as an EAB female, but must also have the 3-dimensional shape and small-scale surface texture found on the elytra.

7 Concluding remarks

Here we have applied bionic-engineering concepts to fabricate polymeric visual decoys in order to lure emerald ash borers and other invasive pest species in the genus *Agrilus*. This procedure involves the stamping of a PET sheet with two dies directly replicated from a dead EAB female, after coating the PET sheet with polymer layers to achieve a structural color that is close to the color of the elytra of the EAB. The procedure is industrially scalable as nearly a hundred decoys were produced from a single biotemplate. Field testing of the visual decoys was carried out and preliminary results show them to be more effective than dead EAB females for attracting overflying beetles. The ineffectiveness of control traps with unstamped silhouettes of the EAB demonstrated that the visual decoys must have not only the iridescent green coloration but also the structure of the EAB elytra.

Although the small sample size in this study was sufficient to illustrate the concept that artificial visual decoys are effective to lure EAB males for entrapment, field tests with a smaller variety of decoys and a much larger number of traps are planned for the next opportune EAB season in order to better ascertain the efficacy of the visual decoys.

Acknowledgments

We thank Miklós Toth and Zoltan Imrei (Hungarian Academy of Sciences) and György Csóka (Hungarian Forest Research Institute) for assistance with locating field sites. Funding for this work was provided in part by USDA-APHIS-CPHST Cooperative Agreement No. 11-8130-0081-CA. Akhlesh Lakhtakia acknowledges ongoing support for his research from the Charles Godfrey Binder Endowment at Penn State. Raúl J. Martín-Palma thanks Banco de Santander for financial support.

References

- [1] Haack R A, Jendek E, Liu H, Marchant K R, Petrice T R, Poland T M, Ye H. The emerald ash borer: A new exotic pest in North America. *Newsletter of the Michigan Entomological Society*, 2002, **47**, 1–5.
- [2] Poland T M, McCullough D G. Emerald ash borer: Invasion of the urban forest and the threat to North America's ash resource. *Journal of Forestry*, 2006, **104**, 118–124.
- [3] Lelito J P, Fraser I, Mastro V C, Tumlinson J H, Böröczky K, Baker T C. Visually mediated 'paratrooper copulations' in the mating behavior of *Agrilus planipennis* (Coleoptera: Buprestidae), a highly destructive invasive pest of North American ash trees. *Journal of Insect Behavior*, 2007, **20**, 537–552.
- [4] Lelito J P, Fraser I, Mastro V C, Tumlinson J H, Baker T C. Novel visual-cue-based sticky traps for monitoring of emerald ash borers, *Agrilus planipennis* (Col., Buprestidae). *Journal of Applied Entomology*, 2008, **132**, 668–674.
- [5] Crook D J, Francese J A, Zylstra K E, Fraser I, Sawyer A J, Bartels D W, Lance D R, Mastro V C. Laboratory and field response of the emerald ash borer (Coleoptera: Buprestidae), to selected regions of the electromagnetic spectrum. *Journal of Economic Entomology*, 2009, **102**, 2160–2169.
- [6] Pulsifer D P, Lakhtakia A, Kumar J, Baker T C, Martín-Palma R J. Toward pest control via mass production of realistic decoys of insects. *Proceedings of SPIE*, 2012, **8339**, 83390H.
- [7] Pulsifer D P, Lakhtakia A. Background and survey of bio-replication techniques. *Bioinspiration and Biomimetics*, 2011, **6**, 031001.
- [8] Pulsifer D P, Lakhtakia A, Martín-Palma R J, Pantano C G. Mass fabrication technique for polymeric replicas of arrays of insect corneas. *Bioinspiration and Biomimetics*, 2010, **5**, 036001.
- [9] Dushkina N, Lakhtakia A. Structural colors, cosmetics and fabrics. *Proceedings of SPIE*, 2009, **7401**, 740106.
- [10] Extrand C W. Spin coating of very thin polymer films. *Polymer Engineering and Science*, 1994, **34**, 390–394.
- [11] Bailey J, Sharp J S. Thin film polymer photonics: Spin cast distributed Bragg reflectors and chirped polymer structures. *European Physical Journal E*, 2010, **33**, 41–49.
- [12] Martín-Palma R J, Pantano C G, Lakhtakia A. Biomimetization of butterfly wings by the conformal evaporated-film-by-rotation technique for photonics. *Applied Physics Letters*, 2008, **93**, 083901.
- [13] Shaler R C, Lakhtakia A, Rogers J W, Pulsifer D P, Martín-Palma R J. Columnar-thin-film acquisition of fingerprint topology. *Journal of Nanophotonics*, 2011, **5**, 051509.
- [14] Pulsifer D P, Lakhtakia A, Martín-Palma R J. Improved

- conformal coatings by oblique-angle deposition for bio-replication. *Applied Physics Letters*, 2009, **95**, 193701.
- [15] McGeough J A, Leu M C, Rajurkar K P, De Silva A K M, Liu Q. Electroforming process and application to micro/macro manufacturing. *CIRP Annals—Manufacturing Technology*, 2001, **50**, 499–514.
- [16] Lenau T, Barfoed M. Colours and metallic sheen in beetle shells—A biomimetic search for material structuring principles causing light interference. *Advanced Engineering Materials*, 2008, **10**, 299–314.
- [17] Wyszecki G, Stiles W S. *Color Science: Concepts and Methods, Quantitative Data and Formulae, 2nd ed.*, Wiley, New York, 1982.
- [18] Jacobs G H. The distribution and nature of colour vision among the mammals. *Biological Reviews*, 1993, **68**, 413–471.
- [19] Cicerone C M, Hoffman D D, Gowdy P D, Kim J S. The perception of color from motion. *Perception & Psychophysics*, 1995, **57**, 761–777.
- [20] Domingue M J, Csóka G, Tóth M, Véték G, Péntes B, Mastro V, Baker T C. Field observations of visual attraction of three European oak buprestid beetles toward conspecific and heterospecific models. *Entomologia Experimentalis et Applicata*, 2011, **140**, 112–121.